Title
Temperature and radiation effects at the fluorine K-edge in LiF

Authors
Schwartz, Craig P
Ponce, Francisco
Friedrich, Stephan
et al.

Publication Date
2017-07-01

DOI
10.1016/j.elspec.2017.05.007

Peer reviewed

Journal of Electron Spectroscopy and Related Phenomena 218 (2017) 30–34

Contents lists available at ScienceDirect

Journal of Electron Spectroscopy and Related Phenomena

journal homepage: www.elsevier.com/locate/elspec

Regular Article

Temperature and radiation effects at the fluorine K-edge in LiF

Craig P. Schwartz[a,b], Francisco Ponce[c,d], Stephan Friedrich[c], Stephen P. Cramer[d,e], John Vinson[f], David Prendergast[a,*]

[a] The Molecular Foundry, Lawrence Berkeley National Laboratory, USA
[b] SSRL, SLAC National Accelerator Laboratory, USA
[c] Lawrence Livermore National Laboratory, USA
[d] University of California, Davis, USA
[e] Lawrence Berkeley National Laboratory, USA
[f] National Institute of Standards and Technology, USA

ARTICLE INFO

Article history:
Received 9 July 2016
Received in revised form 28 February 2017
Accepted 24 May 2017
Available online 30 May 2017

Keywords:
NEXAFS
XANES
Rock-salt
Temperature effects

ABSTRACT

The fluorine K-edge of LiF is studied both experimentally and theoretically as a function of temperature. Instantaneous thermal fluctuations in atomic positions are shown in molecular dynamics simulations to increase in amplitude from 0.029 to 0.064 nm in the temperature range from 40 to 298 K. This is sufficient to cause instantaneous deviations from local octahedral atomic symmetry in this rock-salt crystal, resulting in altered electronic structure. The lowered symmetry of the lowest core-excited states of fluorine atoms is evident in X-ray absorption spectra at the F K-edge. In addition, sufficient radiation exposure produces a new X-ray absorption peak, below the F K-edge of LiF, which is assigned to defects in LiF based on both calculations and comparison to previous experiments.

1. Introduction

Lithium fluoride at room temperature and pressure is a simple and well-studied crystal with the rock salt structure [1–3]. It has found applications in optics, radiation detection, and nuclear reactors [4–7]. Herein, we study variations in the near-edge X-ray absorption fine structure (NEXAFS) [8] of this salt with temperature. NEXAFS is an element-specific probe that excites core electrons into available unoccupied orbitals with a dipole selection rule that constrains the overall change in angular momentum about the excited atom. The effects of temperature on X-ray absorption spectra have been discussed previously [9–13]. It was noted that temperature can cause vibrational modes to become excited. This can enhance the intrinsic motion due to zero point effects and lead to noticeable spectral changes.

The NEXAFS of LiF at the fluorine K edge has been investigated previously [14,15]. We show that, even for this simple crystal, a temperature dependence is evident in NEXAFS with spectral changes appearing with increasing temperature. Using first-principles calculations we show that fluctuations in the relative atomic coordinates consistent with thermal motion can give rise to noticeable spectral changes. Additionally, the radiation sensitivity of the crystal is investigated, which is particularly important since LiF is sometimes used as a radiation detector. It is shown that radiation damage results in missing fluorine atoms in the LiF lattice.

2. Materials and methods

A 0.5 μm LiF film was deposited by Lebow Company onto a 200 nm Si_3N_4 window fabricated by Norcada Inc. The LiF film was mounted with double sided carbon tape to the end of a cold finger that can be inserted into a synchrotron endstation and cooled to ~4 K with a helium flow cryostat. We estimate the temperature was ~10 K near the surface of the sample. Electrical contact to the samples was made using silver paint, and samples were loaded into the 2T magnet chamber on beam line 6.3.1 of the Advanced Light Source synchrotron at Lawrence Berkeley National Laboratory. The beamline monochromator has a nominal resolving power (E/ΔE) of 5000 at 700 eV and provides a flux of 5×10^{10} photons/s/0.1%BW for the line density of 600/mm grating.

Fluorine K-edge X-ray absorption spectra of the LiF film were taken by total electron yield using a Keithley picoammeter. The signals were normalized to the incident beam intensity measured with a gold mesh located upstream of the sample, and the energy scale was calibrated based on previous studies [14,15]. Pristine samples were freshly exposed to X-rays, while damaged samples had been

* Corresponding author.
E-mail address: dgprendergast@lbl.gov (D. Prendergast).

http://dx.doi.org/10.1016/j.elspec.2017.05.007
0368-2048/

exposed for several minutes (a minimum of 15 min). A fresh sample spot was used following temperature changes. Total electron yield (TEY) was used due to deviations from Beer's law behavior in transmission mode due to saturation. The experiments were repeated at least five times. The effect of radiation damage was predominantly seen in giving rise to a new peak at low energy. The effects of polarization have previously been shown to be of minimal importance for LiF [15].

We calculated NEXAFS spectra using the OCEAN package [16,17], which generates X-ray absorption spectra by solving the Bethe-Salpeter equation (BSE) within a basis of electron and hole states (and associated core-hole dielectric screening) provided by the Kohn-Sham orbitals of density functional theory (DFT) [18]. The DFT electronic structure was calculated within the generalized gradient approximation using the Quantum ESPRESSO code [19], and efficient numerical sampling of the Brillouin zone was enabled through use of the Shirley interpolation scheme [20,21]. For the final states we included the first 672 conduction bands, from our plane wave DFT calculation, and the screening of the core-hole potential included 2000 bands. For the BSE calculations we used a $5 \times 5 \times 5$ k-point grid and down-sampled the wavefunctions to a $20 \times 20 \times 20$ real-space mesh from a DFT plane wave cut-off of 100 Ry using the Perdew Berke Ernzerhof (PBE) functional within the generalized gradient approximation (GGA) [22]. Calculated LiF F K-edge spectra (p-type transitions) were numerically broadened via convolution with a Lorentzian with half-width half-maximum of 0.272 eV to match the core-hole lifetime. In comparison to the experiment, the overall calculated spectra have a slightly smaller feature spacing due to a lack of a GW correction to counteract the underestimated bandwidth within PBEGGA [23]. The LiF spectra, sampled from molecular dynamics trajectories, are aligned with respect to one another based on total energy differences of the core-excited states; a valid procedure as all simulation cell dimensions and number of atoms are kept constant. A single constant energy shift was applied to these simulated spectra to align them with the experimental data. The LiF defect structure consisted of a single missing F atom in a $3 \times 3 \times 3$ supercell (215 atoms), and the ionic positions were relaxed. The transition energy was determined based on total energy differences as compared to a known standard MgF_2 using the XCH scheme detailed previously [24]. The crystal coordinates of Li and F in LiF were taken from the literature [25], and used as a starting point for generation of distributions of atomic positions at various temperatures. These were sampled from 15 ps DFT PBE GGA molecular dynamics (MD) trajectories generated by the VASP code for a $2 \times 2 \times 2$ cubic supercell (64 atoms) Nosé-Hoover thermostat and used to calculate the relevant spectra [26]. A different simulation was run for each temperature and the snapshots were separated in time by at least 4 picoseconds each. The molecular dynamics simulations agree well with previous simulations [26].

The potential energy surfaces were generated by taking a $3 \times 3 \times 3$ cubic supercell (216 atoms), freezing the atoms on the periphery of the cell to preserve the ground state lattice constant, moving a central fluorine atom along a given lattice vector while allowing the rest of the atoms to relax freely to accommodate the perturbed F atom.

3. Results and discussion

The total electron yield fluorine K-edge absorption spectrum was measured at both room temperature and a nominal 10 K (Fig. 1a). The experimental spectra (dotted lines) are dominated by a large feature centered at ~694 eV and another feature at ~703 eV. There is a low energy shoulder at ~692 eV. Noticeable differences between the warm (purple) and cold (light blue) spectra are that the warm spectrum has a slightly lower energy feature (~692 eV) and the main feature at ~694 eV is both less intense and broader. These variations are consistent with our temperature-dependent simulations (solid lines), in which the feature at ~703 eV becomes broader with increasing temperature (red to orange to yellow to green to blue) due to the resulting increase in the amplitude of atomic motion. There are very minor changes between 0 K and 77 K, with changes becoming noticeable at 198 K, similar to previous simulations of the lithium K-edge [27]. The main peak loses intensity and the spectrum shifts to lower energies at 298 K. An effect is seen in the low energy feature: with increasing temperature in our experiments, this feature is observed to broaden, exhibiting a lower energy absorption onset, as shown in Fig. 1b. Our temperature-dependent simulations indicate both an overall increase in spectral broadening and a new spectral feature (~692 eV) appearing with increasing temperature. This feature grows in the calculated spectra monotonically with increasing temperature. This low energy feature is absent when the atomic positions are locked in their high symmetry octahedral coordination. However, sampling thermal distributions of atomic positions yields this low energy feature, which grows in intensity with increasing temperature. This is due to local atomic symmetry being instantaneously broken by thermal motion, enabling transitions to orbitals that would nominally be forbidden under octahedral coordination of the excited F atom [27].

The appearance of the ~692 eV pre-edge peak can be explained in a manner analogous to previous non-resonant inelastic X-ray scattering (NRIXS) measurements on LiF [14]. By changing the scattering angle in NRIXS, one can increase the contribution to the total absorption intensity to s-like final states at the F K-edge (1 s –> 3 s). These measurements indicate that the F K-edge absorption onset is dominated by excited states with significant s-character about the excited fluorine atom [14,15]. In standard soft X-ray NEXAFS experiments, where photon momentum transfer is negligible and X-ray induced transitions are firmly within the dipole limit, this s-character would preclude the observation of such transitions without invoking some additional mechanism. First-principles simulations indicate that the lowest energy F 1s excited state in LiF results in an exciton that can be factorized into a F 1s hole and an electronic component of predominantly s-character at the excited F atom – consistent with the ideal octahedral coordination. In principle, this optically inaccessible (dark) state should be observable with NRIXS, at finite momentum transfer, without any deviation from octahedral symmetry. In our experiments, with negligible momentum transfer, the pre-edge absorption intensity was triggered instead by temperature-induced structural deviations from octahedral symmetry. This reduces the symmetry of atomic coordination about the excited atom and results in hybridization of the local electronic structure to produce final states with a first-moment, i.e., some p-character to enable dipole-allowed transitions.

This interpretation of the origins of the pre-edge intensity relies on approximating the nuclear degrees of freedom as classical, from the context of the much lighter and faster electrons, which, in the absence of electronic state-crossing, adiabatically evolve on the potential energy surface defined by the nuclear subsystem. The physics embodied within this picture is essentially equivalent to a quantum mechanical interpretation, which would label this pre-edge transition as vibronic in character. Within perturbation theory, the leading order contribution to transition amplitudes of electronically dipole-forbidden transitions reflects the variation of the electronic dipole moment with respect to collective nuclear degrees of freedom (vibrons in the case of isolated systems; phonons in the case of periodic models) – the so-called Herzberg-Teller effect. Previous work has already noted that for light atoms, nuclear displacements at finite temperature (result-

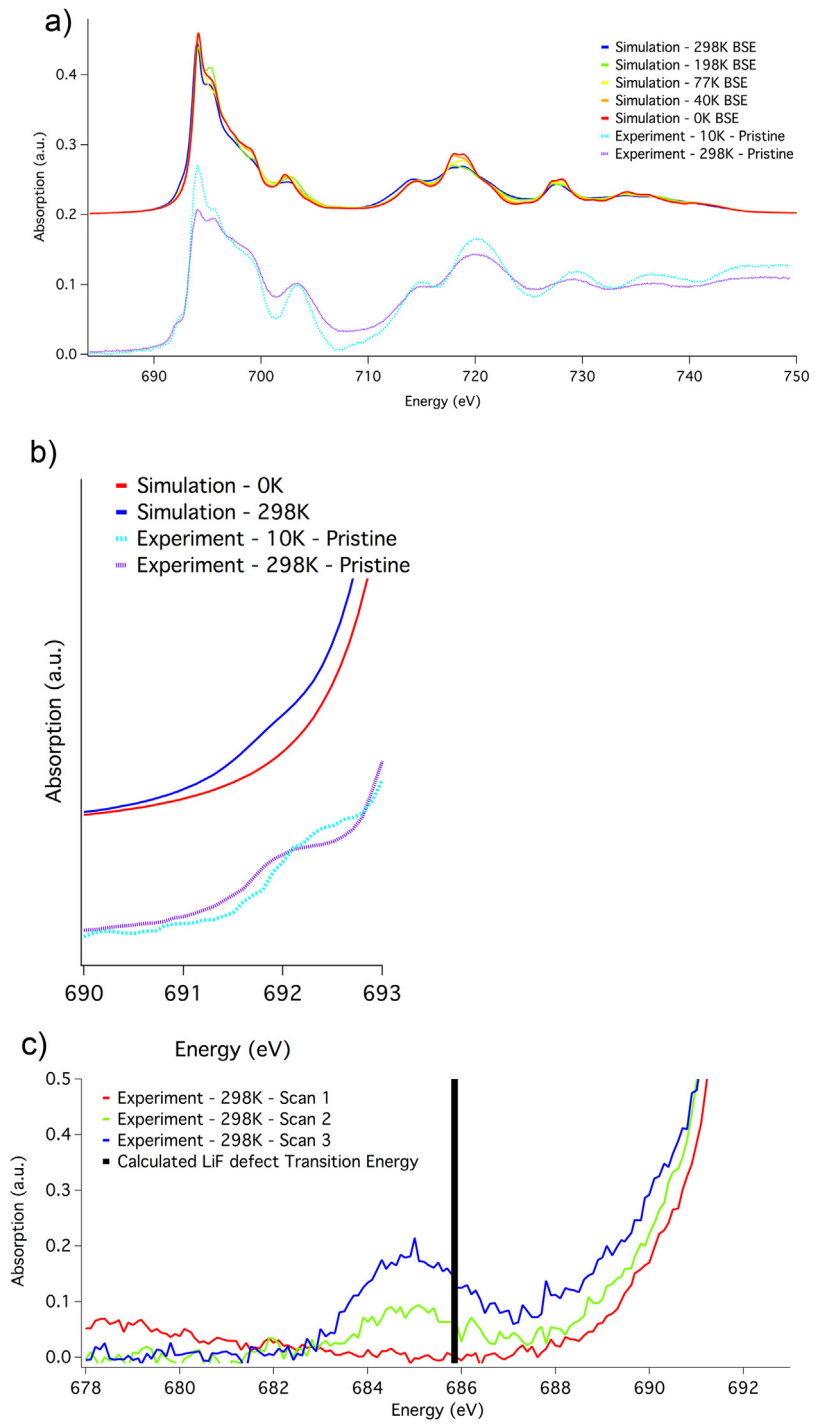

Fig. 1. a) Experimental X-ray Absorption Spectrum at the F K-edge of LiF at 10 K (blue dashed) and 298 K (purple dashed) as compared to spectra calculated at 0 K, 40 K, 77 K, 198 K, and 298 K (red, orange, yellow green, blue solid respectively). With increasing temperature in both experiment and theory there is a lower energy feature present. b) Zoom of pristine low energy feature showing more broadening at higher temperature compared to low temperature for both experiment (298 K purple, 0 K blue) and calculations (0 K red, 298 K blue). The intermediate points show a gradual rise in the feature at ~692 eV. c) Zoom of a low energy pre-edge feature at the F K-edge before that grows in as a result of radiation damage at the F K-edge. Shown are the experimental spectra from a sample exposed at 298 K following repeated exposure to radiation (red, green and blue) in increasing order of radiation exposure. The expected first transition energy of LiF with a missing F atom is shown by the black line. (For interpretation of the references to colour in this figure legend, the reader is referred to the web version of this article.)

ing from incoherent superpositions of the amplitudes of populated vibrons/phonons) are reasonably well-modeled within molecular dynamics by treating the nuclei classically [27,28]. And, the electronic orbital evolution subject to these nuclear degrees of freedom can, in most cases (in the absence of conical intersections etc.), be treated within the Born-Oppenheimer approximation, thereby capturing Herzberg-Teller effects and additional effects beyond the harmonic approximation for nuclear dynamical response. Additional nuclear amplitude, particularly with respect to zero-point motion, resulting from a more accurate inclusion of the quantum degrees of freedom of the nuclei has also been explored in the case of dinitrogen [29].

The interpretation of vibronic features within X–ray absorption spectra has a long history, coupled with advances in high-resolution

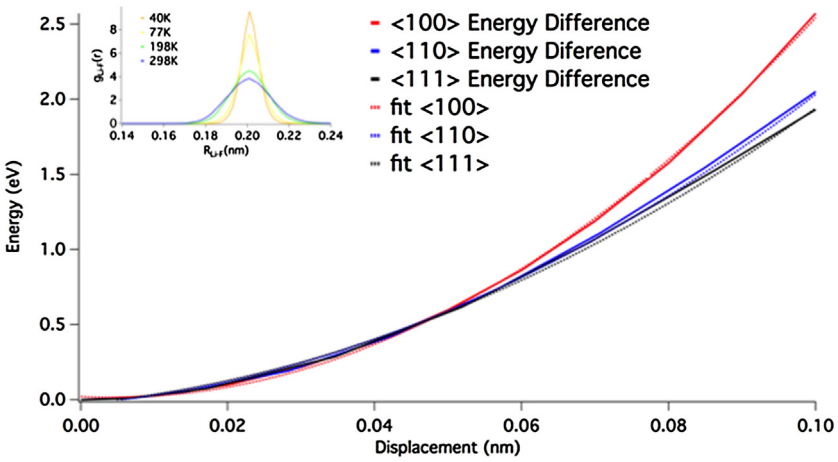

Fig. 2. Plot of potential energy increase vs. displacement distance of a fluorine atom along the specified crystal direction (solid) ⟨100⟩ (red) ⟨110⟩ (blue) and ⟨111⟩ (black) and their associated quadratic fits (dashed). The distribution of Li-F nearest neighbor distances as a function of temperature is shown in the inset. (For interpretation of the references to colour in this figure legend, the reader is referred to the web version of this article.)

measurements of simple molecular systems, such as methane, where the Herzberg-Teller effect was invoked within the harmonic approximation [30]. More recently, studies of carbon dioxide and dinitrogen at high pressure, have successfully interpreted NRIXS by relying on the classical approximation for nuclear degrees of freedom with associated adiabatic electronic evolution [12]. In the solid state context, our pre-edge assignment agrees with numerous other materials studied. In $SrTiO_3$ at the Ti K-edge the effect of temperature was shown to lead to an increase in a similar pre-edge feature [31]. In fact, this effect has been attempted to be generalized both with respect to direct phonon effects captured in DFT and based on nonequilibrium Green's functions [32,33]. The method has been extended to include zero point motion and other quasiharmonic approximations producing an excellent match with experiment for corundum [34]. The phonon-based method accurately describes the temperature effects seen in MgO. This work also showed that XANES can be obtained with reasonable accuracy by averaging together several nonequilbrium spectra, identical to the method used in this work.

The peak at ~694 eV has previously been assigned to the core-exciton peak [14]. The main peak at ~694 eV loses intensity at finite temperature due to the movement of the atoms shifting the position of the peak. This leads to slightly broader and noticeably less intense peak. However, the peak at higher energy is very sensitive to the position of the atoms in a non-trivial fashion. The exact effect causing the peak at ~696 eV to change intensity with disorder is related to complex movements of the overall crystal and cannot be easily assigned. While this feature is correlated with an elongation of one of the Li-F bonds, this is likely not the only cause. The trend is qualitatively in agreement with experiment, the temperature effect is less pronounced in experiment. Perhaps this is due to a lack of major defects such as Frenkel or Schottky defects in the simulated spectra. Such defects would lead to the subtle effects of atomic motion being obscured.

Fig. 1c shows the effect of radiation damage with increasing exposure from red to green to blue. A new feature arises at ~685 eV due to radiation exposure. The transition is consistent with the evolution of defects based on a calculation of the lowest F 1s excited state of LiF with a missing fluorine defect (blue vs. red). The large full width at half maximum (FWHM) of ~1.5 eV is substantially broader than the core-hole lifetime likely due to a large variety of defects present. [35] This is probably further enhanced by creation of F_2 and F_3^+ color centers [36,37]. Note that the peak position and width are similar with other defects found in fluorine samples [38–40].

The connection between increasing temperature and this pre-edge spectral feature can be rationalized from Fig. 2. For all F atom is displacement directions, the computed potential energy surface exhibits a quadratic dependence (to a good approximation). Based on a Boltzmann populated vibrational harmonic oscillator with a frequency of 38.0 meV calculated for the first several hundred states, the population of the first vibrational excited state exhibits ~17.6% occupancy at 298 K, while at 40 K this is reduced to only ~0.0016%. At low temperatures, zero point effects will be important, although these are absent from our molecular dynamics calculations in which ions evolve as classical particles. The inset of Fig. 2 shows the statistical distribution of Li-F separations as a function of temperature sampled from Born-Oppenheimer MD, in which the atomic nuclei are treated as classical particles. The amplitude of the distribution, estimated by the half width at half maximum expands from ~0.029 nm to ~0.064 nm when the temperature is increased from 40 K to 298 K based on a Gaussian fitting, between approximately 1 and 3 percent of the Li-F bond length. However, as was seen in previous work studying Li in LiF, the F distribution is slightly asymmetric at high temperatures, resulting in a two Gaussian fit producing a lower residual error. [27]. Even though the local coordination of F atoms in LiF at 198 K exhibits significant spontaneous deviations from octahedral symmetry – lowering the main-edge intensity at ~694 eV – this does not lead to a noticeable increase in the pre-edge intensity at ~692 eV. Since the origin of the pre-edge feature is related to electronic hybridization between an unperturbed s-state and other orbitals which induce some p-character at this site, and since hybridization typically varies according to the inverse of atomic distance squared within tight-binding models, the data are consistent with linear increases in thermal deviations as a function of temperature which induce non-linear increases in pre-edge intensity proportional to 1/(1-aT) [2]. However, given the relatively few temperature points and the difficulty in accurately extracting the pre-edge peak intensity without other peaks interfering, definitive scaling confirmation awaits further confirmation, ideally on a system with a more distinct (i.e., well-separated) pre-edge.

The strong harmonic nature of the curve, combined with the high symmetry of the rock salt structure implies that a Debye-Waller based approach might work in this case. Indeed, such was the implied conclusion for another rock salt crystal, MgO [41]. A simple analysis shows that at the relatively low temperatures studied here, a Debye-Waller analysis gives a visually similar result. We note that at high enough temperatures the Debye-Waller type anal-

ysis will break down for this system. We expect it should always break down in cases of free rotation and significant anharmonicity.

4. Conclusions

The F K-edge X-ray absorption spectrum of LiF has been measured at both low temperature (10 K) and room temperature. The data show a spectral broadening matched by simulated spectra derived from first-principles molecular dynamics simulations and based on distributions of atomic positions consistent with finite temperature. The thermal motions of atoms within LiF breaks local symmetry and induces noticeable spectral changes due to the perturbation of electronic orbitals with nominally dipole-forbidden transitions. These deviations in atomic separations are smaller than 0.0064 nm, yet this is still large enough to cause noticeable spectral changes. Furthermore, a new feature, well below the absorption edge of LiF, is identified as missing F atoms, produced by radiation damage.

Acknowledgements

We thank the Advanced Light Source Synchrotron at Lawrence Berkeley National Laboratory for providing beam time and Elke Arenholz for her expertise and assistance during the experiment. Part of this work was performed under the auspices of the U.S. Department of Energy by Lawrence Livermore National Laboratory under Contract DE-AC52-07NA27344. The Stanford Synchrotron Radiation Lightsource and Molecular Foundry are National User Facilities operated by Stanford University and the University of California Berkeley for the US Department of Energy, grants DE-AC02-76SF00515 and DE-AC02-05CH11231 respectively. The Molecular Foundry portion of this work was performed under a user proposal with D.P. Certain products are identified in this paper to foster understanding. Such identification does not imply recommendation or endorsement by the National Institute of Standards and Technology, nor does it imply that these are necessarily the best available for the purpose.

References

[1] P. Debye, P. Scherrer, Physikalische Zeitschrift 17 (1916) 277–283.
[2] P.L. Bayley, Phys. Rev. 24 (5) (1924) 495–501.
[3] R.J. Havighurst, Proc. Natl. Acad. Sci. U. S. A. 12 (1926) 477–479.
[4] I.D. Hau, T.R. Niedermayr, O.B. Drury, A. Burger, Z. Bell, S. Friedrich, Nucl. Instrum. Methods Phys. Res. Sect. A-Accel. Spectrom. Dect. Assoc. Equip. 559 (2) (2006) 745–747.
[5] J.I. Larruquert, J.A. Aznarez, L. Rodriguez-de Marcos, J.A. Mendez, A.M. Malvezzi, A. Giglia, P. Miotti, F. Frassetto, G. Massone, S. Nannarone, G. Crescenzio, G. Capobianco, S. Fineschi, Damage to Vuv, Euv, and X-Ray Optics Iv; and Euv and X-Ray Optics: Synergy between Laboratory and Space Iii, vol. 8777, 2013, pp. 10.
[6] C.S. Sona, B.D. Gajbhiye, P.V. Hule, A.W. Patwardhan, C.S. Mathpati, A. Borgohain, N.K. Maheshwari, Corros. Eng. Sci. Technol. 49 (4) (2014) 287–295.
[7] T. Yanagida, N. Kawaguchi, Y. Fujimoto, K. Fukuda, K. Watanabe, A. Yamazaki, A. Uritani, J. Lumin. 144 (2013) 212–216.
[8] J. Stöhr, NEXAFS Spectroscopy, Springer, 1992.
[9] C. Brouder, D. Cabaret, A. Juhin, P. Sainctavit, Phys. Rev. B 81 (11) (2010) 115125.
[10] A. Lévy, F. Dorchies, A. Benuzzi-Mounaix, A. Ravasio, F. Festa, V. Recoules, O. Peyrusse, N. Amadou, E. Brambrink, T. Hall, M. Koenig, S. Mazevet, Phys. Rev. Lett. 108 (5) (2012) 055002.
[11] D. Manuel, D. Cabaret, C. Brouder, P. Sainctavit, A. Bordage, N. Trcera, Phys. Rev. B 85 (22) (2012) 224108.
[12] J. Inkinen, A. Sakko, K.O. Ruotsalainen, T. Pylkkanen, J. Niskanen, S. Galambosi, M. Hakala, G. Monaco, S. Huotari, K. Hamalainen, Phys. Chem. Chem. Phys. 15 (23) (2013) 9231–9238.
[13] T. Pylkkänen, A. Sakko, M. Hakala, K. Hämäläinen, G. Monaco, S. Huotari, J. Phys. Chem. B 115 (49) (2011) 14544–14550.
[14] K. Hamalainen, S. Galambosi, J.A. Soininen, E.L. Shirley, J.P. Rueff, A. Shukla, Phys. Rev. B 65 (15) (2002) 5.
[15] E. Hudson, E. Moler, Y. Zheng, S. Kellar, P. Heimann, Z. Hussain, D.A. Shirley, Phys. Rev. B 49 (6) (1994) 3701–3708.
[16] J. Vinson, J.J. Rehr, J.J. Kas, E.L. Shirley, Phys. Rev. B 83 (11) (2011) 7.
[17] K. Gilmore, J. Vinson, E.L. Shirley, D. Prendergast, C.D. Pemmaraju, J.J. Kas, F.D. Vila, J. Rehr, J. Comput. Phys. Commun. 197 (2015) 109–117.
[18] W. Kohn, L.J. Sham, Phys. Rev. 140 (4A) (1965), 1133-&.
[19] P. Giannozzi, S. Baroni, N. Bonini, M. Calandra, R. Car, C. Cavazzoni, D. Ceresoli, G.L. Chiarotti, M. Cococcioni, I. Dabo, A. Dal Corso, S. de Gironcoli, S. Fabris, G. Fratesi, R. Gebauer, U. Gerstmann, C. Gougoussis, A. Kokalj, M. Lazzeri, L. Martin-Samos, N. Marzari, F. Mauri, R. Mazzarello, S. Paolini, A. Pasquarello, L. Paulatto, C. Sbraccia, S. Scandolo, G. Sclauzero, A.P. Seitsonen, A. Smogunov, P. Umari, R.M. Wentzcovitch, J. Phys. -Condes. Matter. 21 (39) (2009) 19.
[20] D. Prendergast, S.G. Louie, Phys. Rev. B 80 (23) (2009) 10.
[21] E.L. Shirley, Phys. Rev. B 54 (23) (1996) 16464–16469.
[22] J.P. Perdew, K. Burke, M. Ernzerhof, Phys. Rev. Lett. 77 (18) (1996) 3865–3868.
[23] E.L. Shirley, Phys. Rev. B 58 (15) (1998) 9579–9583.
[24] T. Yamamoto, T. Mizoguchi, K. Tatsumi, I. Tanaka, H. Adachi, Y. Muramatsu, E.M. Gullikson, R.C.C. Perera, Mater. Trans. 45 (7) (2004) 1991–1993.
[25] Z.H. Sun, J. Dong, Y.W. Xia, Physica B 406 (19) (2011) 3660–3665.
[26] G. Kresse, J. Hafner, Phys. Rev. B 47 (1) (1993) 558–561.
[27] T.A. Pascal, U. Boesenberg, R. Kostecki, T.J. Richardson, T.C. Weng, D. Sokaras, D. Nordlund, E. McDermott, A. Moewes, J. Cabana, D. Prendergast, J. Chem. Phys. 140 (3) (2014) 13.
[28] J.S. Uejio, C.P. Schwartz, R.J. Saykally, D. Prendergast, Chem. Phys. Lett. 467 (2008) 195.
[29] S. Fatehi, C.P. Schwartz, R.J. Saykally, D. Prendergast, J. Chem. Phys. 132 (2010) 094302.
[30] P.S. Bagus, M. Krauss, R.E. LaVilla, Chem. Phys. Lett. 23 (1) (1973) 13–17.
[31] S. Nozawa, T. Iwazumi, H. Osawa, Phys. Rev. B 72 (12) (2005) 4.
[32] R. Nemausat, D. Cabaret, C. Gervais, C. Brouder, N. Trcera, A. Bordage, I. Errea, F. Mauri, Phys. Rev. B 92 (14) (2015) 144310.
[33] T. Fujikawa, H. Sakuma, K. Niki, D. Sebilleau, J. Electron. Spectrosc. Relat. Phenom. 198 (2015) 57–67.
[34] R. Nemausat, B. Ch, G. Ch, D. Cabaret, J. Phys.: Conf. Ser. 712 (1) (2016) 012006.
[35] M.O. Krause, J.H. Oliver, J. Phys. Chem. Ref. Data 8 (2) (1979) 329–338.
[36] A.K. Dauletbekova, A.T. Akilbekov, M.V. Zdorovets, A.A. Abdrahmetova, K.A. Kuterbekov, M.V. Koloberdin, Bull. Karaganda State Univ. Ser. Phys. 1 (2009) 14–21.
[37] R. Larciprete, L. Gregoratti, M. Danailov, R.M. Montereali, I. Bonfigli, M. Kiskinova, Appl. Phys. Lett. 80 (20) (2002) 3862–3864.
[38] F. Cosandey, J.F. Al-Sharab, F. Badway, G.G. Amatucci, P. Stadelmann, Microsc. Microanal. 13 (2) (2007) 87–95.
[39] N. Jiang, J. Qiu, J. Silcox, J. Appl. Phys. 96 (11) (2004) 6230–6233.
[40] A.S. Vinogradov, S.I. Fedoseenko, S.A. Krasnikov, A.B. Preobrajenski, V.N. Sivkov, D.V. Vyalikh, S.L. Molodtsov, V.K. Adamchuk, C. Laubschat, G. Kaindl, Phys. Rev. B 71 (4) (2005) 11.
[41] R. Nemausat, D. Cabaret, C. Gervais, C. Brouder, N. Trcera, A. Bordage, I. Errea, F. Mauri, Phys. Rev. B 92 (14) (2015) 12.